# The Scattering and Neutrino Detector at the LHC

Giovanni De Lellis[1,2]⋆

**1** Dipartimento di Fisica "E. Pancini", Università di Napoli "Federico II", via Cintia 19, 80126, Napoli, Italy
**2** Istituto Nazionale di Fisica Nucleare, via Cintia 19, 80126, Napoli, Italy
* giovanni.de.lellis@cern.ch

September 26, 2022

## Abstract

**SND@LHC, Scattering and Neutrino Detector at the LHC, is a compact experiment designed to perform measurements with neutrinos produced at the LHC in the unexplored pseudo-rapidity region of $7.2 < \eta < 8.4$, complementary to all the other experiments at the LHC. The experiment was approved in March 2021. It was constructed in about one year and it is now taking data during the Run 3 of the LHC. In this paper we review the detector concept, the physics case and the status of the data taking.**

## 1 Introduction

As the accelerator with the highest beam energy, the LHC is also the source of the most energetic human-made neutrinos. Indeed, the LHC produces an intense and strongly collimated beam of TeV-energy neutrinos along the direction of the proton beams.

Already in 1984, De Rujula and Rückl proposed to use the LHC neutrino beam by placing a neutrino experiment in the far forward direction [1]. This idea of detecting LHC neutrinos was revisited several times in the following decades [2, 3]. More recently, a feasibility study was carried out, resulting in the estimate of the physics potential and in the identification of a proper location underground in the LHC tunnel for such an experiment to operate during the Run3 of the LHC [4, 5]. The SND@LHC Collaboration submitted a Letter of Intent in August 2020 [6] and a Technical Proposal in January 2021 [7].

## 2 Experiment concept

The experiment is located 480 m downstream of IP1 in the TI18 tunnel, an injection tunnel during LEP operation. The detector consists of a hybrid system based on an 830 kg target mass of tungsten plates, interleaved with emulsion and electronic trackers, followed downstream by an hadronic calorimeter and a muon identification system, as shown in Figure 1. The emulsion films with their micrometric accuracy [8] constitute the vertex detector while trackers in the target region, based on the Scintillating Fibre technology [9], provide the time stamp to

the events and complement emulsion for the electromagnetic energy reconstruction. Nuclear emulsion films are readout by state-of-the-art, fully automated, optical scanning systems [10–13]. The hadronic calorimeter and muon system comprises eight layers of scintillating bar planes interleaved with 20 cm-thick iron slabs. The three most downstream stations are made of fine grained bars with both horizontal and vertical orientation, to trace the penetrating muons. Every scintillating bar as well as every fibre module is viewed by SiPMs.
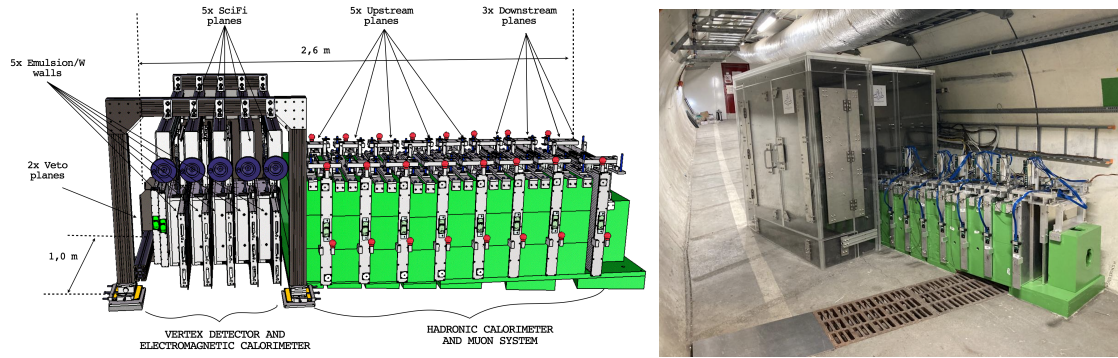


Figure 1: Detector layout (left) and picture of the detector installed in TI18 (right).

The detector configuration allows efficiently distinguishing between all three neutrino flavours, as well as searching for Feebly Interacting Particles via signatures of scattering in the detector target [14]. The first phase aims at operating the detector throughout Run 3 to collect about 290 fb$^{-1}$.
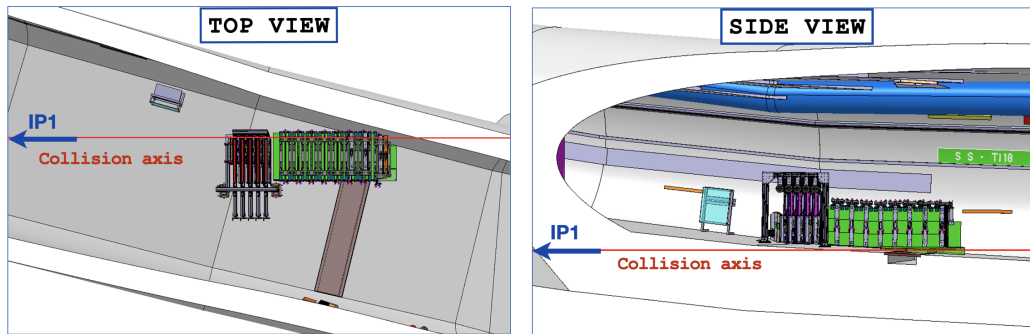


Figure 2: Side and top views of the SND@LHC detector in the TI18 tunnel [7].

The detector takes full advantage of the space available in the TI18 tunnel to cover the desired range in pseudo-rapidity. Figure 2 shows the top and side views of the detector positioned inside the tunnel. The energy measurement and the muon identification set a constraint on the minimum length of the detector. With the constraints from the tunnel, this requirement competes with the azimuthal angular acceptance that determines the overall flux intercepted and therefore the total number of observed interactions. The combination of position and size of the proposed detector is an optimal compromise between these competing requirements. The geometrical constraints also restrict the detector to the first quadrant only around the nominal collision axis, as shown in the top view of the detector in Figure 2.

The result is a compact detector, 2.6 m in length. The energy measurement and the muon identification limit the target region to a length of about 80 cm. The transverse size down-

stream of about 80(H) × 60(V) cm$^2$ is limited by the constraint of the tunnel side wall. The transverse size of the target region is proportionally smaller in order to match the acceptance of the energy measurement and the muon identification for the vertices identified in the target volume. In order to maximise the number of neutrino interactions, tungsten has been selected as the passive material. The emulsion target will be replaced a few times per year.

With data from Run 3, SND@LHC will be able to study more than two thousand high-energy neutrino interactions.

All the detector systems were constructed in the labs by Summer 2021 and were assembled and tested at CERN. On November 1st, the installation underground started. A borated polyethylene shielding box was added to surround the target and absorb low-energy neutrons originated from beam-gas interactions as shown in the right picture of Figure 1. The detector installation was completed on April 7$^{th}$th 2022 by adding the target walls with emulsion films, and it is now taking data with the Run 3 of the LHC.

We review in the following the physics case of the experiment.

## 2.1 QCD measurements

Electron neutrinos in $7.2 < \eta < 8.4$ range are mostly produced by charm decays. Therefore, $\nu_e$s can be used as a probe of charm production in an angular range where the charm yield has a large uncertainty, to a large extent coming from the gluon parton distribution function (PDF). Electron neutrino measurements can thus constrain the uncertainty on the gluon PDF in the very small (below $10^{-5}$) $x$ region. The interest therein is two-fold: gluon PDF in this $x$ domain will be relevant for Future Circular Collider (FCC) detectors; secondly, the measurement will reduce the uncertainty on the flux of very-high-energy atmospheric neutrinos produced in charm decays, essential for the evidence of neutrinos from astrophysical sources [15, 16]. The charm measurement in Run3 will be affected by a systematic uncertainty at the level of 30% and by a statistical uncertainty of 5%.

The left plot of Figure 3 shows the ratio between charm measurements in different $\eta$ regions normalised to the LHCb measurement [17]: gluon PDF uncertainty provides the largest contribution. SND@LHC will measure charm in the $7.2 < \eta < 8.4$ region where the PDF uncertainty is dominant.

## 2.2 Lepton flavour universality with neutrino interactions

In the pseudo-rapidity range of interest, tau neutrinos are essentially only produced in $D_s \to \tau \nu_\tau$ and the subsequent $\tau$ decays. One can thus assume that the source of both $\nu_e$ and $\nu_\tau$ is essentially provided by semi-leptonic and fully leptonic decays of charmed hadrons. Unlike $\nu_\tau$s produced only in $D_s$ decays, $\nu_e$s are produced in the decay of all charmed hadrons. Therefore, the $\nu_e / \nu_\tau$ ratio depends only on the charm hadronisation fractions and decay branching ratios. The systematic uncertainties due to the charm-quark production mechanism cancel out, and the ratio becomes sensitive to the $\nu$-nucleon interaction cross-section ratio of the two neutrino species. The measurement of this ratio can thus be considered a lepton flavour universality (LFU) test in $\nu$ interactions. Charmed hadron fractions and $\nu$ branching ratios produce a systematic uncertainty on this ratio of about 22% while the statistical uncertainty is dominated by the low statistics of the $\nu_\tau$ sample,, with a 30% accuracy [7].

LFU can also be tested with the $\nu_e$ to $\nu_\mu$ ratio. $\nu_\mu$s are much more abundant but contaminated by $\pi$ and $K$ decays, and therefore the production mechanism cannot be considered the same as for $\nu_e$s. However, this contamination is mostly at low energies. Above 600 GeV, the contamination is reduced to about 35%, and stable with the energy. Moreover, charmed hadron decays have practically equal branching ratios into $\nu_e$s and $\nu_\mu$s. As a result, the $\nu_e / \nu_\mu$ ratio provides a test of the LFU with an uncertainty of 15% [7].
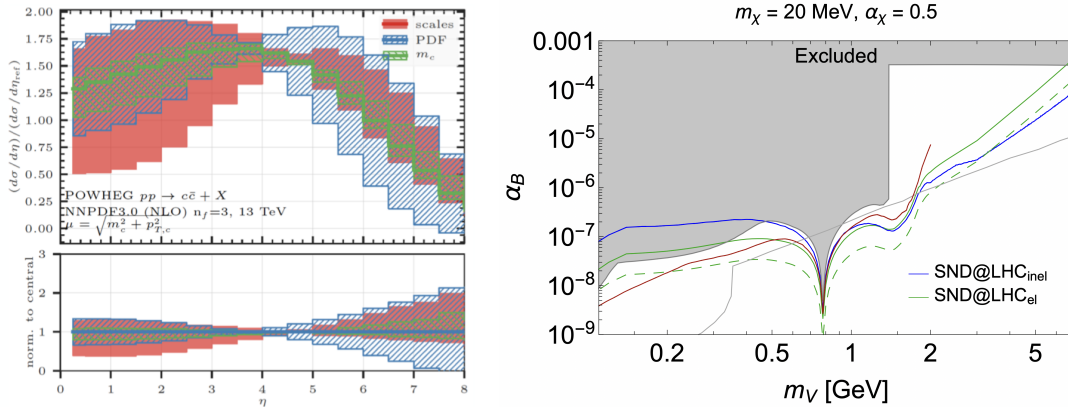
Figure 3: Left: Ratio between the differential cross-section at 13 TeV and the differential cross-section at 7 TeV, with the latter evaluated in the pseudo-rapidity range $4 < \eta < 4.5$ [7]. Right: Sensitivity of the SND@LHC experiment to the leptophobic portal [14]

## 2.3 Feebly Interacting Particles

The experiment is also capable of performing model-independent direct searches for FIPs. A recent work [14] summarises the experiment sensitivity to physics beyond the Standard Model, by considering the scatterings of light dark matter particles $\chi$ via leptophobic $U(1)_B$ mediator, as well as decays of Heavy Neutral Leptons, dark scalars and dark photons.

SND@LHC is unique in its capability to perform a direct dark matter search at accelerators. The right plot of Figure 3 shows the sensitivity of the experiment to the leptophobic portal under the assumption that $m_\chi = 20$ MeV and the coupling of the mediator to $\chi$ particles is $\alpha_\chi = 0.5$. The considered signatures are the elastic scattering off protons (green line, 10 signal events) and the deep-inelastic scattering (blue line, 100 signal events). The dashed line corresponds to the upgraded setup that may operate during Run 4. The red line shows the 100 event contour for the DUNE experiment [18].

## 3 Outlook

The experiment is now taking data during the Run 3 of the LHC and the full apparatus is being commissioned with collision data. While a few small independent emulsion bricks exposed during the LHC commissioning have already been developed, indicating a negligible background level, the collaboration is starting the analysis of the first set of emulsion from the target region. The extraction of the emulsion and the installation of a fully instrumented detector were successfully done at the end of July, halfway through the LHC intensity ramp-up. In the meantime, data from the electronics detector are continuously analysed. A new era of collider neutrinos has just started.

## References

[1] A. De Rujula and R. Ruckl, *Neutrino and muon physics in the collider mode of future accelerators*, In *SSC Workshop: Superconducting Super Collider Fixed Target Physics*, pp. 571–596, doi:10.5170/CERN-1984-010-V-2.571 (1984).

[2] A. De Rujula, E. Fernandez and J. Gomez-Cadenas, *Neutrino fluxes at future hadron colliders*, Nucl. Phys. B **405**, 80 (1993), doi:10.1016/0550-3213(93)90427-Q.

[3] H. Park, *The estimation of neutrino fluxes produced by proton-proton collisions at $\sqrt{s} = 14$ TeV of the LHC*, JHEP **10**, 092 (2011), doi:10.1007/JHEP10(2011)092, 1110.1971.

[4] S. Buontempo, G. M. Dallavalle, G. De Lellis, D. Lazic and F. L. Navarria, *CMS-XSEN: LHC Neutrinos at CMS. Experiment Feasibility Study* (2018), 1804.04413.

[5] N. Beni *et al.*, *Physics Potential of an Experiment using LHC Neutrinos*, J. Phys. G **46**(11), 115008 (2019), doi:10.1088/1361-6471/ab3f7c, 1903.06564.

[6] SND@LHC Collaboration, *Scattering and Neutrino Detector at the LHC*, Tech. rep., CERN, Geneva (2020).

[7] C. Ahdida *et al.*, *SND@LHC - Scattering and Neutrino Detector at the LHC*, Tech. rep., CERN, Geneva (2021).

[8] C. W. Fabjan and H. Schopper, eds., *Particle Physics Reference Library: Volume 2: Detectors for Particles and Radiation*, Springer Nature, Cham, ISBN 978-3-030-35317-9, 978-3-030-35318-6, doi:10.1007/978-3-030-35318-6 (2020).

[9] LHCb Collaboration, *LHCb Tracker Upgrade Technical Design Report*, Tech. rep. (2014).

[10] A. Alexandrov *et al.*, *A new fast scanning system for the measurement of large angle tracks in nuclear emulsions*, JINST **10**(11), P11006 (2015), doi:10.1088/1748-0221/10/11/P11006.

[11] A. Alexandrov *et al.*, *A new generation scanning system for the high-speed analysis of nuclear emulsions*, JINST **11**(06), P06002 (2016), doi:10.1088/1748-0221/11/06/P06002.

[12] A. Alexandrov *et al.*, *The Continuous Motion Technique for a New Generation of Scanning Systems*, Sci. Rep. **7**(1), 7310 (2017), doi:10.1038/s41598-017-07869-3.

[13] A. Alexandrov, G. De Lellis and V. Tioukov, *A Novel Optical Scanning Technique with an Inclined Focusing Plane*, Sci. Rep. **9**(1), 2870 (2019), doi:10.1038/s41598-019-39415-8.

[14] A. Boyarsky, O. Mikulenko, M. Ovchynnikov and L. Shchutska, *Searches for new physics at SND@LHC*, JHEP **03**, 006 (2022), doi:10.1007/JHEP03(2022)006, 2104.09688.

[15] A. Bhattacharya *et al.*, *Prompt atmospheric neutrino fluxes: perturbative QCD models and nuclear effects*, JHEP **11**, 167 (2016), doi:10.1007/JHEP11(2016)167, 1607.00193.

[16] Y. S. Jeong *et al.*, *Neutrinos from charm: forward production at the LHC and in the atmosphere*, PoS **ICRC2021**, 1218 (2021), doi:10.22323/1.395.1218, 2107.01178.

[17] R. Aaij *et al.*, *Measurements of prompt charm production cross-sections in pp collisions at $\sqrt{s} = 13$ TeV*, JHEP **03**, 159 (2016), doi:10.1007/JHEP03(2016)159, [Erratum: JHEP 09, 013 (2016), Erratum: JHEP 05, 074 (2017)], 1510.01707.

[18] S. Naaz, J. Singh and R. B. Singh, *DUNE prospect for leptophobic dark matter*, Advances in High Energy Physics **2020**, 1 (2020), doi:10.1155/2020/9047818.